MedCrave
Step into the World of Research
International Journal of Petrochemical Science & Engineering

Review Article

Open Access

CrossMark

Effects of geometry, temperature, and inlet conditions on the flow split in spheroids manifold

Abstract

A Computational Fluid Dynamics CFD study was conducted on the mal-distribution problem occurring within the pipe network upstream of pairs of spheroids gravity separators used in the oil industry. The series of simulations were conducted using the Euler-Euler multiphase and the k-ε turbulence models. The cases studied reflect different scenarios of oil production capacity in addition to the effect of seasonal variations of temperature increasing from 10°C during winter to 24°C during summer. The inlet conditions were varied so that they permitted to elucidate the effects of the flow rates and temperatures at the inlet of the piping network on the multiphase flow behavior and hence the mal-distribution within the pairs of spheroids considered. Two manifold configurations were taken from real installations in the oil industry. They contain T-junctions with different orientations. Averages of 2.2 million computational cells were generated for each case studied.

The main source of mal-distribution was found to be the sequence and cascading of the existing T-junctions inside the pipe network that are known to act like phase separators. A mal-distribution between the risers of each spheroid was, also, noticed. The relatively large number of T-junctions used, as well as the structure of the downstream piping network employed, led to complex multiphase flow behavior. The mal-distribution, generated by different flow scenarios, were less than 12 for the manifold referred to as Configuration 1. Configuration 2 caused more noticeable mal-distribution reaching up to 40%. The symmetry of the piping networks and the arrangement of the T-junctions were found to be a key parameter among the causes of the mal-distribution.

Keywords: spheroids, T-junction, flow mal-distribution, multiphase flow, CFD

Volume 1 Issue 4 - 2016

Nabil Kharoua, Lyes Khezzar
Department of Mechanical Engineering, The Petroleum Institute, United Arab Emirates

Correspondence: Nabil Kharoua, Department of Mechanical Engineering, The Petroleum Institute, United Arab Emirates, Tel +97126075416, Fax +97126075220, Email nkharoua@pi.ac.ae

Received: October 27, 2016 | **Published:** December 30, 2016

Nomenclature

CD Drag coefficient

d Droplet diameter

D Pipe diameter

f Drag function

gi Acceleration of gravity in the i direction

Gk Turbulent kinetic energy production term

Kpq Interphase exchange coefficient

k Turbulent kinetic energy

p Pressure

Re Reynolds number

S1, S2, S4, S5 Spheroids

N1, N2, N3, N4 Risers

Ui, Uj xi, xj mean velocity component

xi, xj Cartesian coordinates

Greek symbols

α Volume fraction

ε Turbulent kinetic energy Dissipation rate

μ Dynamic laminar viscosity

μt Dynamic turbulent viscosity

ρ Density

σk, σε Prandtl coefficient associated with k and ε respectively

$\bar{\bar{\tau}}_q$ Stress-strain tensor

τp Particle relaxation time

Introduction

Phase separation is a key operation in the oil industry. Crude oil usually contains oil, water, gas, and some other minor components such as solids and salt. Oil and gas should be as pure as possible to match the international standards for hydrocarbons commercialization.[1] The separation process is done by means of large settling devices among which batteries of spheroids are placed downstream of low pressure LP separators. The piping network connecting the spheroids to the LP separators causes a mal-distribution of the crude within each pair of spheroids leading to an overloading of one of the spheroids and an under-loading of the other. The finite volume technique within the framework of the Reynolds averaged Navier-Stokes (RANS) equations and the k-e turbulence model with an Eulerian-Eulerian multiphase model was used to capture the complex behavior of the gas, oil, and water constituting the crude oil. A geometry reflecting the piping network causing the mal-distribution problem was built and

decomposed in finite volumes to solve the set of equations governing the multiphase flow.

The potential sources of unequal split of the mixture are Tee-junctions inside the piping networks. Multiphase flow distribution inside T-junctions is challenging to predict and has been the subject of several previous experimental studies. It is noteworthy to mention that almost all of the existing literature is related to the nuclear and power industry. Pao et al.[2] stated that the work of Orange[3] was the first study on irregular distribution of phases at the pipe junctions. There is consensus within the research community that the main parameters affecting the flow split inside a T-junction are: the geometry (dimensions and orientation of the side arm), inertia differences of the phases, gravity effects, and the flow pattern upstream of the T-junction.[4–6]

It should be mentioned that the majority of the previous studies considered laboratory test cases of T-junctions without complex pipe networks downstream as encountered in industry and which might represent an additional important source of resistance to the flow changing remarkably the flow split trend inside the junction. Azzopardi & Whalley[4] after studying the effect of the different parameters affecting the flow split inside T-junctions, recommended that two-phase flows should not be passed through T-junctions and manifolds unless a very severe mal-distribution of phases at outlet is tolerated. Azzopardi[7] mentioned the importance of the rest of the system downstream of the T-junction on the multiphase flow split behavior. Hart et al.[8] have explained that the liquid route preference is dictated by the balance between forces due to pressure drop (driving force) and due to axial momentum. The research study stated, hence, that for high flow rates, the liquid would prefer the straight trajectory inside the T while, for low flow rates, it would penetrate more easily in the T branch. Recently, research studies explored the possibility to use T-junctions in serial as efficient pre-separation tools.[9] The idea was to use a horizontal pipe connected to a first vertically upward side arm followed by a vertically downward side arm. This has permitted to reach gas-rich product stream containing less than 10 % by volume liquid over a wide range of inlet conditions. This emphasizes the effects that T-junctions can have on upstream approaching multiphase flow with dramatic consequences on flow distributions.

In the present CFD study the Eulerian-Eulerian multiphase model in conjunction with the k-ε turbulence model were used to simulate the multiphase flow behavior inside the pipe network upstream of pairs of spheroids. Several geometrical combinations with different inlet conditions were investigated. The cases studied reflect different scenarios of oil production capacity in addition to the effect of seasonal variations of temperature increasing from 10°C during winter to 24°C during summer. The inlet conditions were varied so that they permitted to elucidate the effects of the flow rates and temperatures at the inlet of the piping network on the multiphase flow behavior and hence the mal-distribution within the pairs of spheroids considered. The CFD approach adopted is presented in the next section including the geometry of the installations, the mathematical models, and the boundary conditions. Subsequently, the results of the simulation cases are illustrated and discussed followed by the conclusions summarized in the last section.

Numerical approach

This section describes the methodology of the present numerical simulation work. The geometrical configurations, the governing equations, the boundary conditions are presented in detail.

a. Manifold configuration

A sketch of a pair of spheroids is presented in Figure 1. The upstream manifold constitutes a complex configuration due to the use of fittings especially T-junctions.

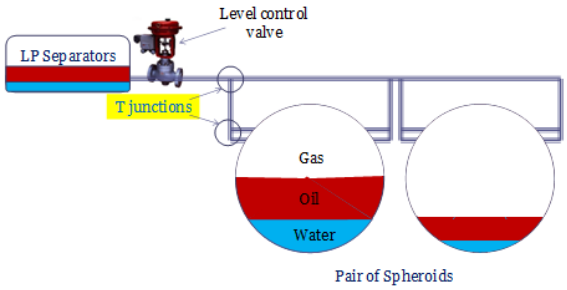

Figure 1 Sketch of the piping network.

The geometry of the pipe network was built in multi-blocks and meshed with a hybrid (98 % hexahedral and 2 % tetrahedral) grid. An average of 2.2 million cells was generated for each case studied. This corresponds to the upper limit of the computational resources available. The two different configurations considered in the present work are shown in Figure 2 and an example of the mesh used is illustrated in Figure 3.

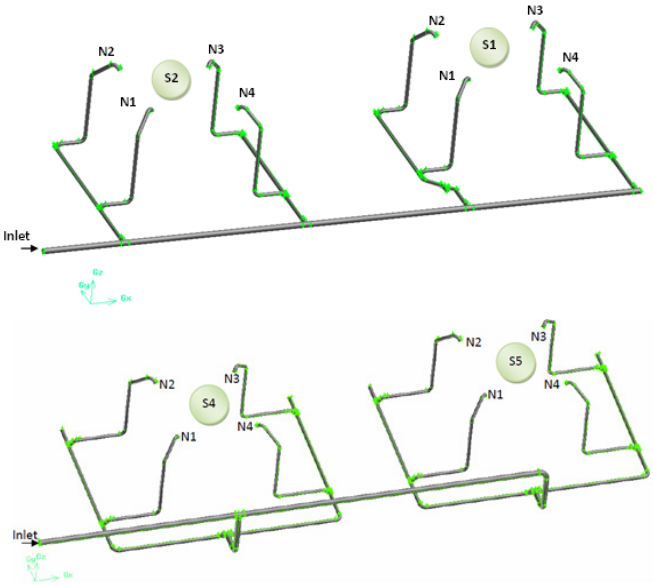

Figure 2 Geometry of the pipe network upstream of the spheroids: top) configuration 1, bottom) configuration2.

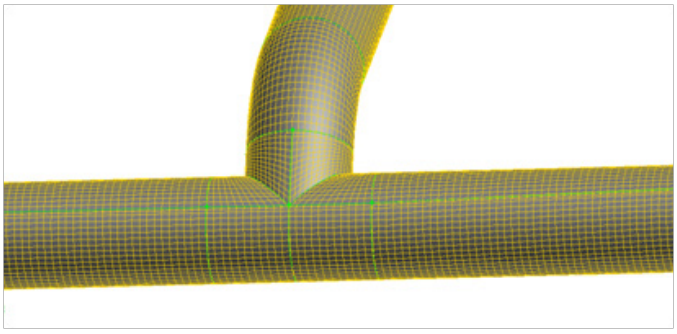

Figure 3 Computational grid: zoom in one of the risers' T-junction.

Citation: Kharoua N, Khezzar L. Effects of geometry, temperature, and inlet conditions on the flow split in spheroids manifold. *Int J Petrochem Sci Eng.* 2016;1(4):106–113. DOI: 10.15406/ipcse.2016.01.00022

b. Eulerian-Eulerian multiphase model

The discretize form of the continuity and momentum equations, for each phase q, are solved to obtain the individual flow fields and volume fractions of each phase. The multiphase continuity equation is

$$\frac{\partial}{\partial x_i}\left(\alpha_q \rho_q U_{i,q}\right) = 0 \qquad \text{…….. (1)}$$

With the condition that $\sum_{k=1}^{n} \alpha_k = 1$

The momentum equations for each phase are defined as

$$\frac{\partial p}{\partial x_i} + \frac{\partial}{\partial x_j}\left(\bar{\bar{\tau}}_q\right) + \alpha_q \rho_q g_i + \sum_{p=1}^{n} \vec{R}_{pq} \qquad \text{……. (2)}$$

Where the stress-strain for the q_{th} phase is modeled as

$$\bar{\bar{\tau}}_q = \alpha_q \mu_q \left(\frac{\partial}{\partial x_j} U_{i,q} + \frac{\partial}{\partial x_i} U_{j,q}\right) + \alpha_q \frac{2}{3} \mu_q \delta_{ij} \frac{\partial}{\partial x_k} U_{k,q} \qquad \text{…… (3)}$$

And the interaction force model between phases $\vec{R}_{pq}$ is

$$\sum_{p=1}^{n} \vec{R} pq = \sum_{p=1}^{n} K_{pq}\left(\vec{U}_p - \vec{U}_q\right) \qquad \text{…… (4)}$$

K_{pq} Is the Interphase exchange coefficient and is equal to

$$K_{pq} = \frac{\alpha_q \alpha_p \rho_p f}{\tau_p} \qquad \text{…….(5)}$$

The particulate relaxation time is defined as

$$\tau_p = \frac{\rho_q d_p^2}{18 \mu_q} \qquad \text{…… (6)}$$

Where f is the drag function

$$\frac{24\left(1+0.15\,\mathrm{Re}^{0.687}\right)}{\mathrm{Re}} \quad \mathrm{Re} \le 1000 \qquad 0.44 \quad \mathrm{Re} > 1000 \qquad \text{……. (7)}$$

And CD is the drag coefficient which according to [10] is

$$\frac{24\left(1+0.15\,\mathrm{Re}^{0.687}\right)}{\mathrm{Re}} \quad \mathrm{Re} \le 1000 \qquad 0.44 \quad \mathrm{Re} > 1000 \qquad \text{……. (8)}$$

The relative Reynolds number for primary phase q and secondary phase p is

$$\mathrm{Re} = \frac{\rho_q \left|\vec{U}_p - \vec{U}_q\right| d_p}{\mu_q} \qquad \text{…….. (9)}$$

Additional forces, such as lift and virtual mass, were neglected. The lift force is due mainly to velocity gradients of the primary phase and is exerted on large secondary-phase liquid droplets. It is not appropriate for closely packed droplets as it is the case for the multiphase flow studied and is insignificant compared to the drag force. Regarding the virtual mass force, it should be added when the density of the secondary phase (oil and water in our case) is much smaller than that of the primary phase (gas in our case).

The relative Re for secondary phase's p and r is

$$\mathrm{Re} = \frac{\rho_{rp} \left|\vec{U}_r - \vec{U}_p\right| d_{rp}}{\mu_{rq}} \qquad \text{…….. (10)}$$

Since the flow is multiphase, the turbulence model should take in consideration the phases contributions and interactions. The turbulence model chosen considers the mixture as a single fluid which characteristic turbulent variables are injected into the individual phase momentum equations. The differential equations for the prediction of the turbulent kinetic energy k and its dissipation rate ε have the form

$$\frac{\partial}{\partial x_j}\left(\rho_m U_{m,j} k\right) = \frac{\partial}{\partial x_j}\left(\frac{\mu_{t,m}}{\sigma_k} \frac{\partial}{\partial x_j} k\right) + G_{k,m} + \rho_m \varepsilon \qquad \text{…….. (11)}$$

$$\frac{\partial}{\partial x_j}\left(\rho_m U_{m,j} \varepsilon\right) = \frac{\partial}{\partial x_j}\left(\frac{\mu_{t,m}}{\sigma_\varepsilon} \frac{\partial}{\partial x_j} \varepsilon\right) + \frac{\varepsilon}{k}\left(C_{1\varepsilon} G_{k,m} - C_{2\varepsilon} \rho_m \varepsilon\right) \qquad \text{…… (12)}$$

Where the mixture density is defined as

$$\rho_m = \sum_{i=1}^{N} \alpha_i \rho_i \qquad \text{…… (13)}$$

The mixture velocity as

$$U_m = \frac{\sum_{i=1}^{N} \alpha_i \rho_i U_i}{\sum_{i=1}^{N} \alpha_i \rho_i} \qquad \text{…… (14)}$$

And the mixture viscosity as

$$\mu_{t,m} = \rho_m C_\mu \frac{k^2}{\varepsilon} \qquad \text{…….. (15)}$$

The production term of k is

$$G_{k,m} = \mu_{t,m}\left(\frac{\partial}{\partial x_j} U_{i,q} + \frac{\partial}{\partial x_i} U_{j,q}\right) \frac{\partial}{\partial x_j} U_{i,q} \qquad \text{…….. (16)}$$

C1ε=1.44, C2ε=1.92, Cμ=0.09, σk=1, σε=1.3

The relatively fine mesh and the set of individual phase equations necessitated to run the simulation in parallel mode using 8 processors for each case. The study employed the commercial code Fluent 12.1.

The Phase-Coupled SIMPLE algorithm was used for pressure-velocity coupling.[10] The convection terms of the momentum, k, and ε equations were discretize using the second order upwind scheme while the QUICK scheme is employed for the volume fraction equation.

c. Boundary conditions

Individual mass flow rates of the phases constituting the crude mixtures were imposed at the inlets with Reynolds numbers, based on the inlet velocity and the pipe diameter D=0.743m, in the range 106-3.7x106 while a pressure condition was prescribed at the outlets. A no-slip condition with a standard wall function[11] was employed at the wall boundaries. Boundary conditions and fluid properties of the reference winter, summer, and modified production scenario cases are detailed in Tables 1-6 for both configurations.

Citation: Kharoua N, Khezzar L. Effects of geometry, temperature, and inlet conditions on the flow split in spheroids manifold. *Int J Petrochem Sci Eng.* 2016;1(4):106–113. DOI: 10.15406/ipcse.2016.01.00022

The modified production scenario case data correspond to the temperature of the summer season. The same fluid composition of the winter case was used at higher temperatures of about 24.82°C to test the temperature effects expected during the summer season with the same production capacity, these cases with higher temperatures will be referred to in the present work as summer case.

Tables 7, Tables 8 summarize the differences between the input data for the cases studied taking as reference the winter case.

Table 1 Boundary conditions-configuration 1-winter case.

	Inlet flow rate (Kg/S)	Inlet flow rate (M3/S)	Volume fraction (%)	Outlet pressure (Pa)	Density (Kg/M3)	Viscosity (Kg/Ms)	Fluid temp(˚C)
Oil	391.2	0.47	10.11	15175	831.4	3.51E-04	12.38
Water	10.66	0.01	0.23		1017	1.22E-04	
Gas	8.73	4.17	89.67		2.092	8.37E-06	

Table 2 Boundary conditions-configuration 1-summer case

	Inlet flow rate (Kg/S)	Inlet flow rate (M3/S)	Volume fraction (%)	Outlet pressure (Pa)	Density (Kg/M3)	Viscosity (Kg/Ms)	Fluid temp. (˚C)
Oil	386	0.468	6.67	15175	825.12	2.87E-04	24.82
Water	10.55	0.01	0.15		1007.5	8.94 E-05	
Gas	14.06	6.533	93.18		2.15	8.42E-06	

Table 3 Boundary conditions-configuration 1-modified production scenario case

	Inlet flow rate (Kg/S)	Inlet flow rate (M3/S)	Volume fraction (%)	Outlet pressure (Pa)	Density (Kg/M3)	Viscosity (Kg/Ms)	Fluid temp. (˚C)
Oil	449.58	0.54	9.2	15175	825.12	2.87E-04	24.82
Gas	11.46	5.33	90.8		2.15	8.42E-06	

Table 4 Boundary conditions-configuration 2-winter case

	Inlet flow rate (Kg/S)	Inlet flow rate (M3/S)	Volume fraction (%)	Outlet pressure (Pa)	Density (Kg/M3)	Viscosity (Kg/Ms)	Fluid temp. (˚C)
Oil	579.03	0.71	11.31		816.98	3.72E-03	
Water	54.67	0.05	0.86	13775	1017.99	1.27 E-03	10.67
Gas	11.18	5.50	87.83		2.03	8.73E-06	

Table 5 Boundary conditions-configuration 2-summer case

	Inlet flow rate (Kg/S)	Inlet flow rate (M3/S)	Volume fraction (%)	Outlet pressure (Pa)	Density (Kg/M3)	Viscosity (Kg/Ms)	Fluid temp. (˚C)
Oil	571.42	0.71	7.22		809.24	2.93E-04	
Water	54.49	0.05	0.55	13775	1007.52	8.96E-05	24.74
Gas	19	9.02	92.22		2.1	8.73E-06	

Table 6 Boundary conditions-configuration 2-modified production scenario case

	Inlet flow rate (Kg/S)	Inlet flow rate (M3/S)	Volume fraction (%)	Outlet pressure (Pa)	Density (Kg/M3)	Viscosity (Kg/Ms)	Fluid temp (˚C)
Oil	244.96	0.3	7.32		809.24	2.93E-04	24.74
Gas	8.03	3.82	92.72	13775	2.1	8.73E-06	

Citation: Kharoua N, Khezzar L. Effects of geometry, temperature, and inlet conditions on the flow split in spheroids manifold. *Int J Petrochem Sci Eng.* 2016;1(4):106–113. DOI: 10.15406/ipcse.2016.01.00022

Table 7 Comparison of the inlet conditions of configuration 1.

Flow rate	Winter case (Kg/S)	Modified production scenario case (Kg/S)	Change in %	Summer case (Kg/S)	Change in %
Oil	391.2	449.6	14.92	385.99	-1.33
Water	10.66	28.7	169.2	10.55	-1.05
Gas	8.73	11.5	31.21	14.06	60.94

Table 8 Comparison of the inlet conditions of configuration 2.

Flow rate	Winter case (Kg/S)	Modified production scenario case (Kg/S)	Change in %	Summer case (Kg/S)	Change in %
Oil	579.03	244.96	-57.69	571.42	-1.31
Water	54.67	15.64	-71.4	54.49	-0.32
Gas	11.18	8.03	-28.12	18.97	69.67

Table 9 Configuration 1: summary of the results.

Case	First spheroid S2 (%)	Second spheroid S1 (%)	Description	Mal-distribution (%)
Winter	53	47	- Reference case	6
Summer	49	51	- Higher gas inflow	2
Modified production scenario	46	54	- Higher inflow	8

Results and discussion

Results and discussion must illustrate and interpret the results of the study. The mal-distribution is illustrated through a mass balance count between the inlet and the outlets of each case. Furthermore, a mass balance for the risers of each spheroid is also considered. An investigation of the possible reasons of the multiphase flow split behavior inside the T-junctions is conducted based on details of the internal flow structure. Simulations using only two phases Tables 3, Tables 6 have shown that the small amount of water can be omitted without any noticeable effect on the final solution of the simulation. The winter production conditions are taken as a reference case.

a. Effects of geometry (winter case)

Configuration 1 is characterized by reduced horizontal side arms of the T-junctions connected to the header. The remaining T-junctions feeding the risers have an upward inclination of 45°C.

Smoglie & Reimann[12] have described the phenomena occurring during the passage of a stratified flow through a horizontal T-junction and have determined what they called the beginning of gas and liquid entrainment corresponding to certain flow conditions. In addition, Azzopardi & Smith[13] concluded that reduced T-junctions can cause much more pronounced phase redistribution as it is the case for the present work.

Relying on the existing literature, although limited for laboratory scale, explanations of the multiphase flow behavior inside both configurations are presented in this section considering the winter case boundary conditions.

Configuration 1 Figure 4 presents almost 10% (gas) mal-distribution between S1 and S2. However a considerable mal-distribution between the risers is observed. A discrepancy of about 5 % in mass balance was observed for the liquid phases.

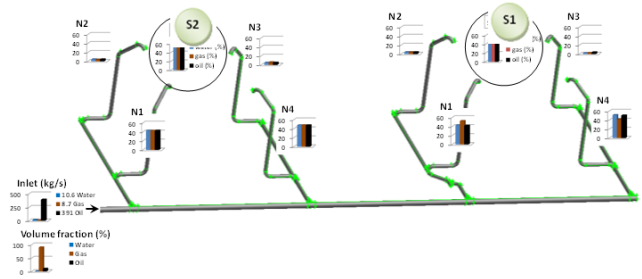

Figure 4 Distribution of crude components (Configuration 1- winter case).

Configuration 2 Figure 5 generates a mal-distribution reaching about 20% between S4 and S5. Contrary to Configuration 1, the distribution within the risers of each spheroid is quasi-homogenous.

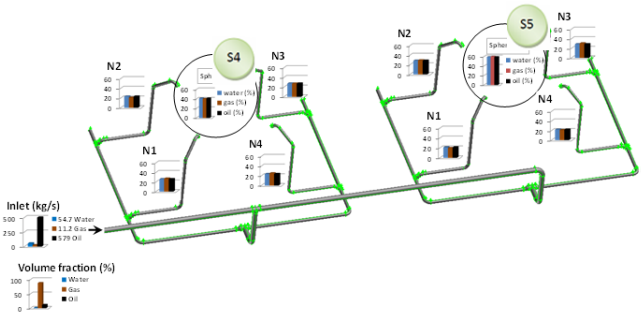

Figure 5 Distribution of crude components (Configuration 2 - winter case).

Figure 6 shows the oil volume fraction distribution inside the whole domain in addition to the four T-junctions connected to the header for configuration 1. The oil-liquid stratification is clearly seen at the last junction however it is not evident at the first one. The risers, containing less fluid (N2 and N3) for both spheroids, are characterized

Citation: Kharoua N, Khezzar L. Effects of geometry, temperature, and inlet conditions on the flow split in spheroids manifold. *Int J Petrochem Sci Eng.* 2016;1(4):106–113. DOI: 10.15406/ipcse.2016.01.00022

by an accumulation of the liquid phase increasing, thus, the resistance effect and pushing the fluids towards the other risers. At the first junction, where no evident stratification is seen, the oil seems to be still dispersed inside the side arm while at the last junction, stratification is noticed inside the side arm. The velocity field, illustrated in Figure 7, shows clearly that any accumulation of liquid seen in Figure 6 is related to a decay of the velocity leading to a more noticeable gravitational effect compared to the inertial momentum.

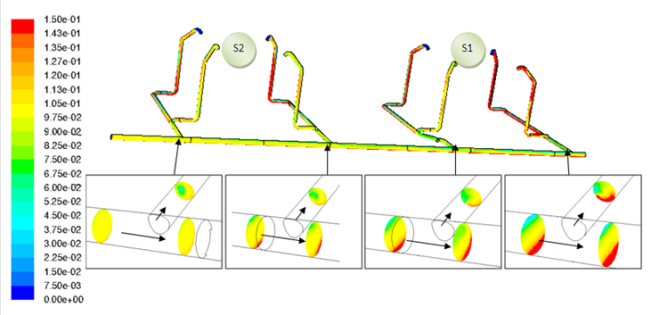

Figure 6 Contours of oil volume fraction distribution for configuration 1 (winter case).

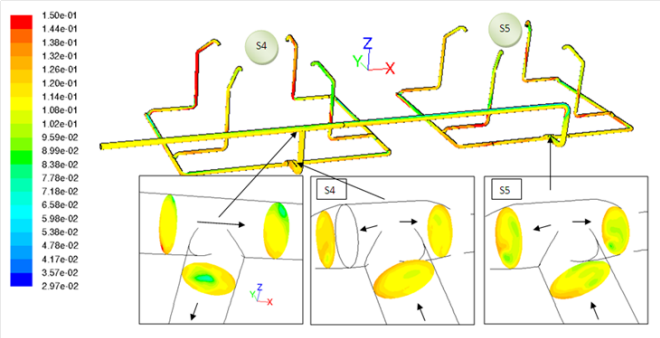

Figure 7 Contours of oil volume fraction distribution for Configuration 2 (winter case).

Contours of the oil volume fraction distribution, inside Configuration 2 Figure 8, show a blockage effect due to the recirculation zone generated in the branch Figure 9.

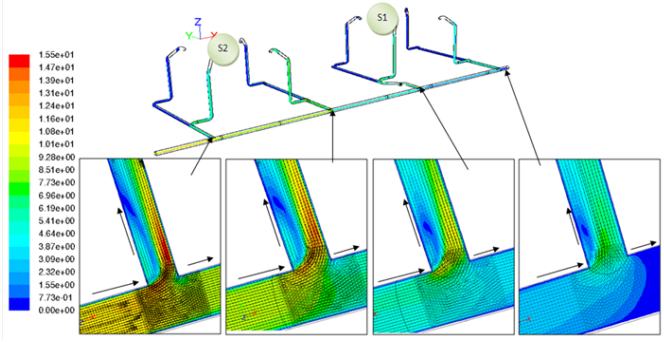

Figure 8 Contours and vectors of velocity magnitude for Configuration 1 (winter case).

This configuration contains a vertically downward side arm connected to the header constituting the T-junction where the main flow split occurs contrary to Configuration 1 where four T-junctions with horizontal branches are employed. This makes the first T-junction the most important location of flow split and, thus, the main source of mal-distribution.

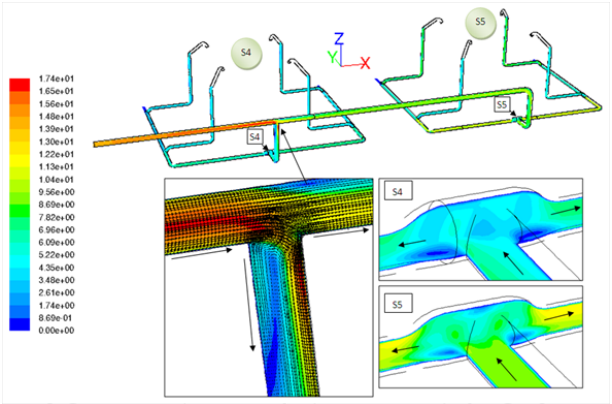

Figure 9 Contours and vectors of velocity magnitude for Configuration 2 (winter case).

b. Effects of temperature

It can be seen from Figure 10 (Configuration 1) that no significant effect of the temperature on the mal-distribution problem is observed. Nonetheless, the behavior of the fluids inside the risers has changed.

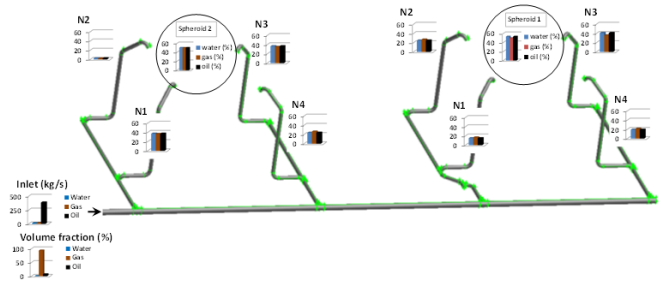

Figure 10 Distribution of crude components (Configuration 1 - summer case).

The trend has completely inverted in the case of S1. In this case only the gas mass flow rate has changed. Again the riser N2 of spheroid S2 inside which almost all fluids are quasi-stagnant correspond to an accumulation of liquid Figure 11 and a decay of the velocity field Figure 12.

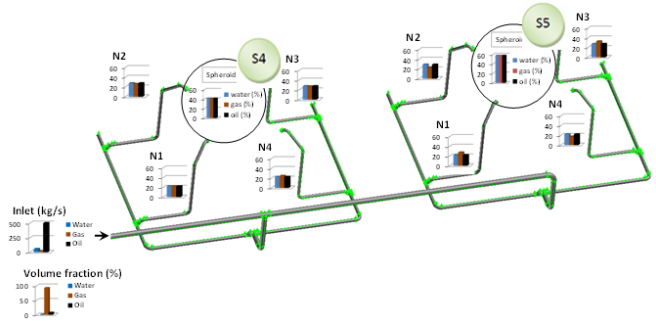

Figure 11 Distribution of crude components (Configuration 2- summer case).

For configuration 2 Figure 13 the mal-distribution trend is similar to that of the winter case. Similarly to Configuration 1, the increase of the gas mass flow rate has delayed, somehow, the stratification of the oil phase inside inlet pipe Figure 14. It was seen (not showed herein) that an appreciable pressure increase occurs in the header just beyond the first T-junction while it decreases remarkably inside the branch.

Citation: Kharoua N, Khezzar L. Effects of geometry, temperature, and inlet conditions on the flow split in spheroids manifold. *Int J Petrochem Sci Eng.* 2016;1(4):106–113. DOI: 10.15406/ipcse.2016.01.00022

The pressure difference between the run and the outlets of S5 is much higher than that between the branch and the outlets of S4 which led to higher velocities inside S5's manifold compared to those inside S4's manifold Figure 15.

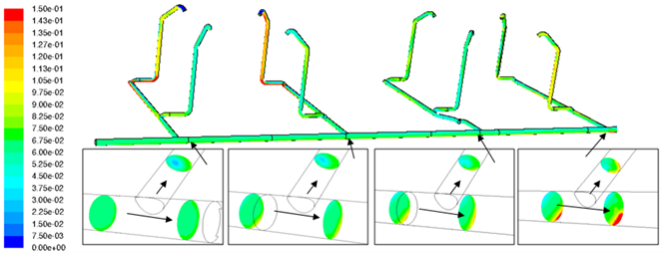

Figure 12 Contours of oil volume fraction distribution for configuration 1 (summer case).

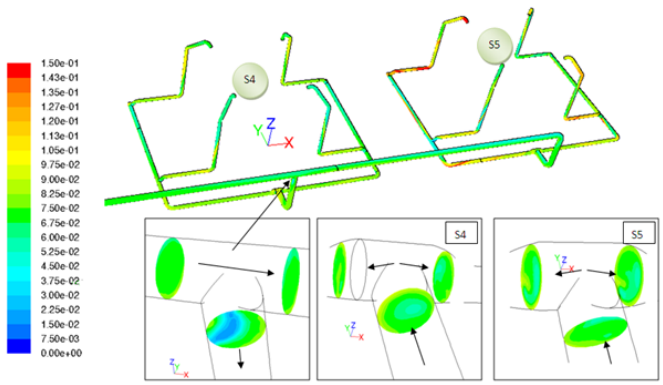

Figure 13 Contours of oil volume fraction distribution for Configuration 2 (summer case).

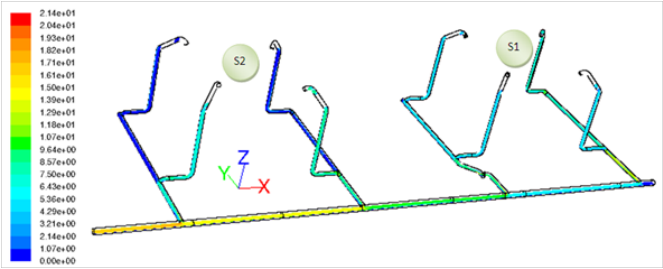

Figure 14 Contours of velocity magnitude for configuration 1 (summer case).

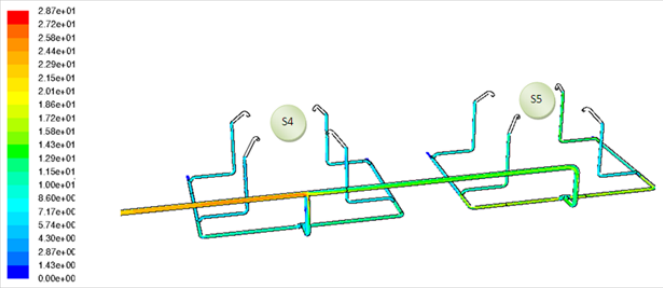

Figure 15 Contours of velocity magnitude for Configuration 2 (summer case).

c. Effects of inlet conditions

The inlet conditions of the modified production scenario case are higher for Configuration 1, in terms of mass flow rates, than those of the winter case Table 7. It was observed that the increase of the gas flow rate only, from winter to summer due to the temperature increase, doesn't affect the trend of the mal-distribution. However, the liquid inlet flow rate has also increased for this case and this is most probably the reason why the mal-distribution trend has inverted making the amount of liquid and gas taken by S1 higher than that taken by S2 due to the increased axial momentum generated by higher velocities inside the header Figure 16. An accumulation of quasi-stagnant oil inside the risers N2 and N3 of S2 was observed corresponding to deceleration of the oil phase and a pressure increase inside the headers.

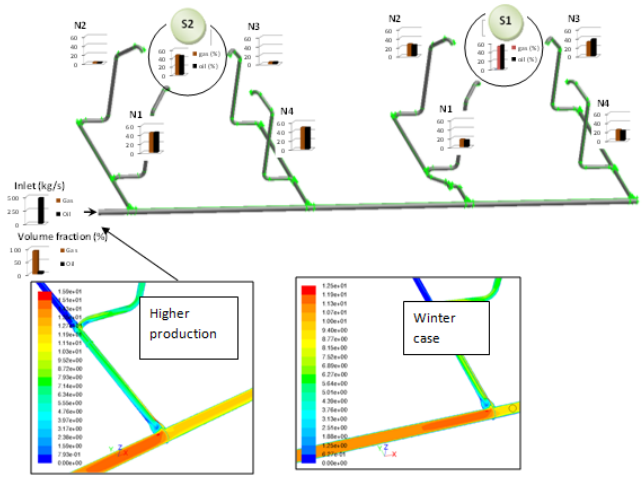

Figure 16 Distribution of crude components (Configuration 1 - modified production scenario case).

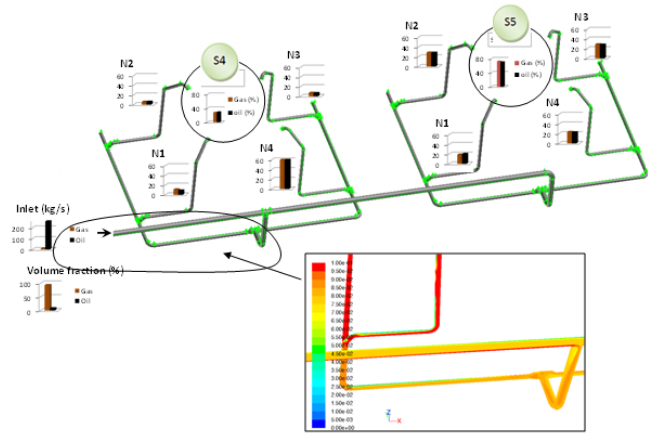

Figure 17 Distribution of crude components (Configuration 2 - modified production scenario case).

For Configuration 2 Figure 17, the same trend, compared with the winter case, was obtained but with a more noticeable mal-distribution reaching 40 %. The amount of fluids leaving the piping network via the risers N1, N2, and N3, of S4, was limited. In fact, there was an accumulation of oil in those risers. This production scenario is 32 % lower than the reference case. Hence, the lower corresponding flow rates at the inlet of the piping network for this case have caused a different multiphase flow behavior inside the risers Table 8.

Tables 9, Tables 10 summarize the main differences, in terms of percentage of liquid accumulated inside each spheroid.

Citation: Kharoua N, Khezzar L. Effects of geometry, temperature, and inlet conditions on the flow split in spheroids manifold. *Int J Petrochem Sci Eng.* 2016;1(4):106–113. DOI: 10.15406/ipcse.2016.01.00022

Conclusion

i. A numerical simulation of the multiphase flow behavior within the piping networks discharging inside spheroids, used in the oil industry as gravity separators, was conducted. The simulations were based on the Eulerian-Eulerian multiphase and the k-ε turbulence models. No accurate field data were available for comparison and total validation of the numerical solution. Nonetheless, the following conclusions can be drawn:

ii. The main source of mal-distribution is the sequence and cascading of the existing T-junctions inside the pipe network that are known to act like phase separators. Existing limited technical literature on the subject of multiphase flow mal-distribution inside T-junctions recommends avoidance of such fittings unless flow mal-distribution can be tolerated.

iii. Several types of T-junctions (with horizontal, upward, and downward branch) were used in the studied configurations leading to a complex multiphase flow behavior and, hence, split.

iv. Configuration 1 generates a mal-distribution less than 12% while, for Configuration 2, important values reaching 40 %, for both gaseous and liquid phases, are reached due to the different geometrical structure of the two piping networks.

v. The liquid flow rate change, at the inlet, affects strongly the mal-distribution trend while the gas flow rate change seems to have relatively negligible effect within the ranges of the present study.

Acknowledgements

The authors of the present work are grateful to the Petroleum Institute of Abu Dhabi for providing High Performance Computing facilities.

Conflict of interest

The author declares no conflict of interest.

References

1. Young GAB, Wakley WD, Taggart DL, et al. Oil–water separation using hydrocyclones:an experimental search for optimum dimensions. *Journal of Petroleum Science and Engineering*. 1994;11(1):37–50.
2. Pao W, Sam B, Nasif MS. Simulation of two phase oil–gas flow in pipeline. *ARPN Journal of Engineering and Applied Sciences*. 2016;11(6):4208–4213.
3. Oranje L. Condensate behavior in gas pipelines is predictable. *Oil & Gas Journal*. 1973;32:39–44.
4. Azzopardi BJ, Whalley PB. The effect of flow patterns on two phase flow in a T–junction. *International Journal of Multiphase Flow*. 1982;17(3):4991–507.
5. Mudde RF, Groen JS, Van Den Akker HEA. Two–phase flow redistribution phenomena in a large T–junction. *International Journal of Multiphase Flow*. 1993;19(4):563–573.
6. Rea S, Azzopardi BJ. The split of horizontal stratified flow at a large diameter T–junction. *Chemical Engineering Research & Design*. 2001;79(4):470–476.
7. Azzopardi BJ. Two–phase flow in junctions. Encyclopedia of Fluid Mechanics. Chap. 1986;25:677–713.
8. Hart J, Hamersrna PJ, Fortuin JMH. Phase distribution during gas/liquid flow through horizontal dividing junctions. *Nuclear Engineering and Design*. 1991;126(3):293–312.
9. Baker G, Clark WW, Azzopardi BJ, et al. Controlling the phase separation of gas–liquid flows at horizontal T–junctions. *AIChE Journal*. 2007;53(8):1908–1915.
10. Schiller L, Naumann Z. A drag coefficient correlation. Deutsch Ing. 1935;77:318–320.
11. Launder BE, Spalding DB. The numerical computation of turbulent flows. Computer Methods in Applied Mechanics and Engineering. 1974;3(2):269–289.
12. Smoglie C, Reimann J. Two–phase flow through small branches in a horizontal pipe with stratified flow. *International Journal of Multiphase Flow*. 1986;12(4):609–625.
13. Azzopardi BJ, Smith PA. Two–phase flow split at T–junctions:effect of side arm orientation and downstream geometry. *International Journal of Multiphase Flow*. 1992;18(6):861–875.